JOURNAL OF APPLIED ELECTROCHEMISTRY **28** (1998) 114–119

Electrocatalysis of oxygen evolution/reduction on $LaNiO_3$ prepared by a novel malic acid-aided method

S. K. TIWARI*‡, J. F. KOENIG‡, G. POILLERAT‡, P. CHARTIER‡, R. N. SINGH*

‡ *Laboratoire d'Electrochimie et de Chimie-Physique du Corps Solide, U.R.A., au CNRS 405, Universite Louis Pasteur, 67000 Strasbourg, France*

* *Electrochemical Laboratory, Department of Chemistry, Faculty of Science, Banaras Hindu University, Varanasi-221 005, India*

Received 18 September 1996; revised 25 March 1997

A kinetic study of the electroformation and electroreduction of oxygen in KOH solutions has been carried out on a $LaNiO_3$ electrode obtained through a malic acid precursor route. The new electrocatalyst was found to show greatly enhanced activity for both oxygen evolution and reduction. The apparent electrocatalytic activity of this electrode for oxygen reduction was more than 10 times higher than those reported for similar electrodes obtained by other methods. It was, however, observed to be less active electrocatalytically for oxygen evolution as compared to the active $LaNiO_3$ electrode obtained by the Bockris–Otagawa coprecipitation method. The electrochemical reaction order with respect to OH^- concentration was found to be approximately 1 in the case of oxygen evolution while that for oxygen reduction, was approximately -1. The Tafel slope values for the reactions were $\sim 2.3\ RT/F$ and $\sim 2 \times 2.3\ RT/3F$, respectively.

Keywords: *$LaNiO_3$ electrode, oxygen electroformation, oxygen electroreduction*

1. Introduction

The electrochemical evolution and reduction of oxygen are of considerable interest [1–3] owing to their use in many electrochemical devices such as secondary metal–air batteries, water electrolysis, chloralkali cells, fuel cells, electrosynthesis and metal electrowinning. The oxygen electrode reaction is, however, known to have high activation overvoltage in aqueous solutions [2] resulting in substantial energy losses. To decrease this activation overvoltage, numerous electrocatalysts have been investigated and extensively reviewed [1–3]. Among these, transition metal mixed oxides, particularly cobalt cobaltite, Co_3O_4, of spinel structure, and binary mixed oxides of La with Ni or Co, of perovskite structure, have been considered most promising and have been intensively studied [4–17]. Of perovskite type oxides, $LaNiO_3$ is of particular interest since it is a metallic conductor ($\rho = 9 \times 10^{-3}\ \Omega\,cm$) at room temperature [18] and can be used as a bifunctional oxygen electrode [19].

In earlier investigations, $LaNiO_3$ was synthesized by a conventional ceramic method or decomposition of solid metal salts, mainly, nitrates [11,12]. These methods required high temperatures and produced oxide powders with small surface area. In recent years, $LaNiO_3$ prepared by other methods, namely, hydroxide solid solution precursor (HSS) [14], spray pyrolysis (SP) [20] and sequential solution coating (SSC) [20, 21] have also been used in the study of the electrocatalysis of oxygen evolution. The latter methods were found to improve the apparent electrocatalytic activity of the catalyst considerably.

Recently, we have synthesized $LaNiO_3$ (LN) via a modified sol–gel process [22] using malic acid (MA) and propionic acid (PA) as complexing agents and investigated its physico-chemical and interfacial electrochemical properties in relation to oxygen evolution in 1 M KOH. Both the new methods yielded pure $LaNiO_3$ in a hexagonal rhombohedral structure with greatly enhanced specific surface area (MA: $17\ m^2\ g^{-1}$; PA: $20\ m^2\ g^{-1}$). The electrocatalytic activity of the catalyst obtained by the former method was higher than that obtained by the latter method. Also, the malic acid method proved to be more advantageous than the propionic acid method, because it produced the pure perovskite phase at a relatively low temperature, 600 °C. We have, therefore, investigated the active $LaNiO_3$ electrode prepared by MA for electrocatalysis of evolution and reduction of oxygen in KOH solutions, the results of which are presented in this paper. Similar studies were not carried out in [22].

2. Experimental details

$LaNiO_3$ was prepared by the malic acid-aided process (MA) as described elsewhere [22]. 35 mmol of each of $La(NO_3)_3.6H_2O$ and $Ni(NO_3)_2.6H_2O$ and 105 mmol of malic acid were dissolved in redistilled water and the volume of solution was made up to 1 dm^3. The pH of the solution was adjusted at 2.5 using 20%

---

* Address for correspondence.

ammonia. This solution was then evaporated to dryness at 110 °C and finally calcined in an electrical furnace at 650 °C for 6 h to obtain the desired oxide.

The oxide powders were transformed to pellet form at 5 ton cm^{-2} pressure, and annealed at 550 °C for 6 h and dipped in 1% polystyrene solution in dichloromethane and then dried at 100 °C [23]. The latter process (dipping and drying) was repeated several times to make the pellet hydrophobic. Finally, one face of the pellet was polished with #1200 emery paper for electrochemical investigations and the other was used for electrical contacts.

Electrochemical studies were carried out at 25 °C in a three electrode conventional Pyrex glass cell having provision for introducing a gas. The steady state E-log i relationships were obtained with a Tacussel potentiostat (type PRT20-2X) and a Minisis 6000 voltmeter (Tacussel). A bright Pt-coil was used as auxiliary electrode. The potential of the test electrode was monitored against a commercial (Tacussel) Hg/HgO/1 M KOH reference electrode.

The electrode kinetic parameters, such as Tafel slope and electrochemical reaction order were determined by carrying out polarization studies under potentiostatic conditions. In the case of O_2 evolution, the oxide electrode was polarized at a higher anodic potential for 10 min and then the potential of the test electrode was decreased in 20 mV steps in the cathodic direction and the corresponding steady value of the current was noted. The time taken for current stabilization was observed to vary with applied potential; it was normally 5–10 min at low overpotentials and 3–4 min at high overpotentials.

In the oxygen reduction study in different KOH solutions, pure O_2 was vigorously bubbled into the electrolyte for 40 min before starting the cathodic polarization and was passed over the electrolyte surface during the experiment. Further, during E/i measurements the test electrode was vibrated at a frequency of 50 Hz by attaching the electrode holder to the diaphragm of a radio speaker [24]. The effect of oxygen partial pressure was also examined in 1 M KOH employing pure oxygen and an oxygen with nitrogen mixture containing 22% oxygen by volume. In this experiment the dissolved oxygen from the electrolyte was first removed by bubbling argon gas into it. After 30 min Ar was replaced by the working gas (O_2 or 22 vol % O_2) which was bubbled through the solution near the test electrode at a constant pressure (1 bar). After 15 min, the steady state cathodic polarization was measured maintaining the condition of the gas bubbling throughout the experiment; the test electrode was kept stationary during the measurements.

3. Results

The iR-corrected steady-state polarization curves for oxygen evolution on a polystyrene-impregnated $LaNiO_3$ electrode at different KOH concentrations (0.25–3 M) are shown in Fig. 1. The current density is based on the geometrical surface area of the electrode. The resistance of the electrode plus the electrolyte (R) was found to be approximately 1 Ω. The Tafel slope values (b) lay between 60 and 68 mV $decade^{-1}$ at low potentials ($E < 650$ mV). The order for oxygen evolution with respect to OH^- ion concentration (p), determined from the slope of the plot, log i against log$[OH^-]$ (Fig. 2) was found to be approximately unity. These results are summarized in Table 1.

Figure 3 shows the steady state cathodic Tafel polarization curves for oxygen reduction in different pre-electrolysed KOH solutions (0.2–1 M). Owing to the observed low reduction current density, the cathodic Tafel curves were not corrected for ohmic contributions. At low potentials ($E < 100$ mV), the value of b for each cathodic Tafel curve was close to 40 mV $decade^{-1}$ and the reaction order in $[OH^-]$ was approximately −1. The latter was determined from the slope of the linear plot, log i against log$[OH^-]$ (Fig. 4). The reaction order with regard to oxygen partial pressure was found to be 0.9 and ~0.5 at low and high overpotentials, respectively. The order

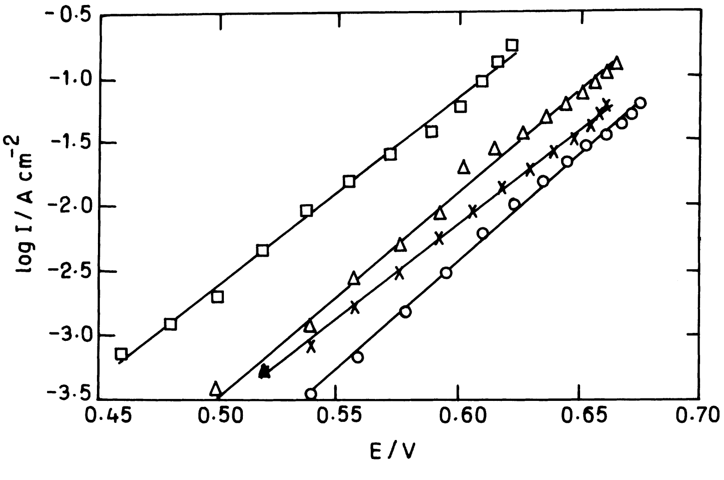

Fig. 1. Tafel plots for oxygen evolution on polystyrene-impregnated $LaNiO_3$ electrode at various KOH concentrations (25 °C): (○) 0.25, (×) 0.5, (△) 1 and (□) 3 M.

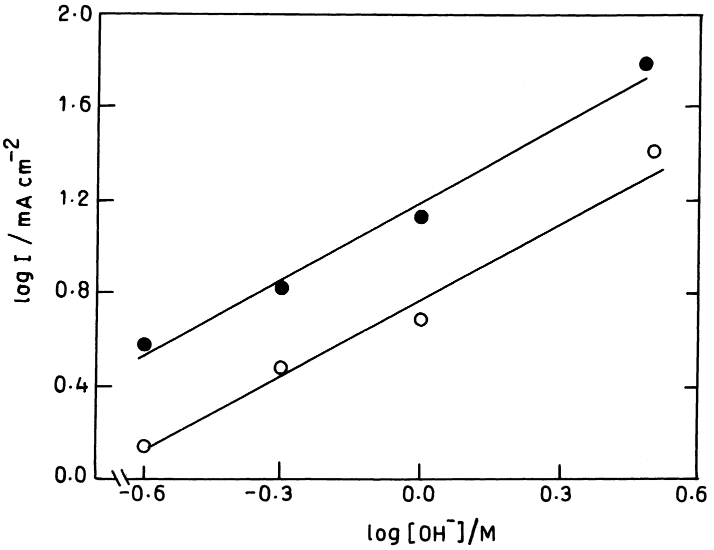

Fig. 2. Plot of log *I* against log [OH$^-$] at constant potentials from Fig. 1. Key: (●) 600 mV; (○) 575 mV.

$[p = (\Delta \log i / \Delta \log p_{O_2})$ at constant potential was estimated from the data shown in Fig. 5.

4. Discussion

It is observed that values of the electrode kinetic parameters for oxygen evolution, namely, the Tafel slope and the reaction order, vary with the method of oxide catalyst preparation [11, 12, 14, 20, 21]. Bockris and Otagawa [11] synthesized $LaNiO_3$ by two different methods, high temperature ceramic and coprecipitation followed by decomposition at 800 °C. The former method gave $b = 65$–130 mV decade^{-1} while the latter gave, 43 mV decade^{-1} up to a current density of 100 mA cm^{-2}. In both cases the electrodes were in the massive pellet form. In contrast, Balej found $b = 95$ mV decade^{-1} [12] on the same oxide prepared by the same Bockris–Otagawa coprecipitation method. Singh *et al.* [14, 20, 21] prepared $LaNiO_3$ in film form by different methods; sequential solution coating [20, 21], oxide–slurry painting [14] and spray pyrolysis [20] and observed $b \approx 60$ mV decade^{-1} in the case of coated films, while that for the sprayed films was only 45 mV decade^{-1}. Also, $LaNiO_3$ prepared *in situ* showed $b \sim 60$ mV decade^{-1} for oxygen evolution.

The observed first order oxygen evolution kinetics in OH$^-$ ion concentration with the polystyrene-impregnated $LaNiO_3$ electrocatalyst is in fair agreement with values previously reported [11, 14, 20, 21]. In some cases, particularly oxygen evolution on $LaNiO_3$ and on Pt/$LaNiO_3$ prepared by coprecipitation [11] and spray pyrolysis [20], respectively, second order kinetics have also been reported.

The electrode kinetic data for oxygen reduction reported in the literature show that the Tafel slope depends on the catalyst preparation method, while the reaction order in [OH$^-$] appears to be independent of it. The *b* values were found to range between 40 and 60 mV decade^{-1} [11, 25–29]. Thus, the observed *b* value (40 mV decade^{-1}) and the reaction order (about −1) for oxygen reduction on LN–MA are in accord with the literature values.

Table 1 shows that among the $LaNiO_3$ electrodes, the electrode LN–MA, with the exception of LN–COP, has the greatest electrocatalytic activity. Its apparent activity in terms of the oxygen evolution current density at $E = 0.625$ V is only two times lower than that of the LN–COP electrode which is presently considered as a highly active oxygen anode. However, the activity of the latter (LN–COP) was reported not to be reproducible [12]. At low overpotential, both the electrodes showed a similar order

Table 1. Comparative values of electrode kinetic parameters for oxygen evolution on $LaNiO_3$ *in 1* M *KOH at 25 °C*

Electrodes	*Roughness factor*, R_F	*Tafel slope* /mV dec^{-1}	*p*	I/mA cm^{-2}			
				0.525 V		0.625 V	
				I_{app}	$I_{tr} \times 10^3$	I_{app}	$I_{tr} \times 10^3$
LN–MA	1500	63	1.1	4.85	3.23	29.10	19.40
LN–C [11]	750	65	1.1	0.55	0.73	1.76	2.35
LN–COP [11]	5600	43	0.95	5.60	1.00	54.00	9.64
Pt/LN–SP [20]	170	45	2.2	0.37	2.18	5.00	29.40
Pt/LN–SSC [20]	470	65	1.2	1.74	3.70	9.40	20.00
Ni/LN–HSS [14]	1820	73	1.2	2.60	1.43	12.30	6.76

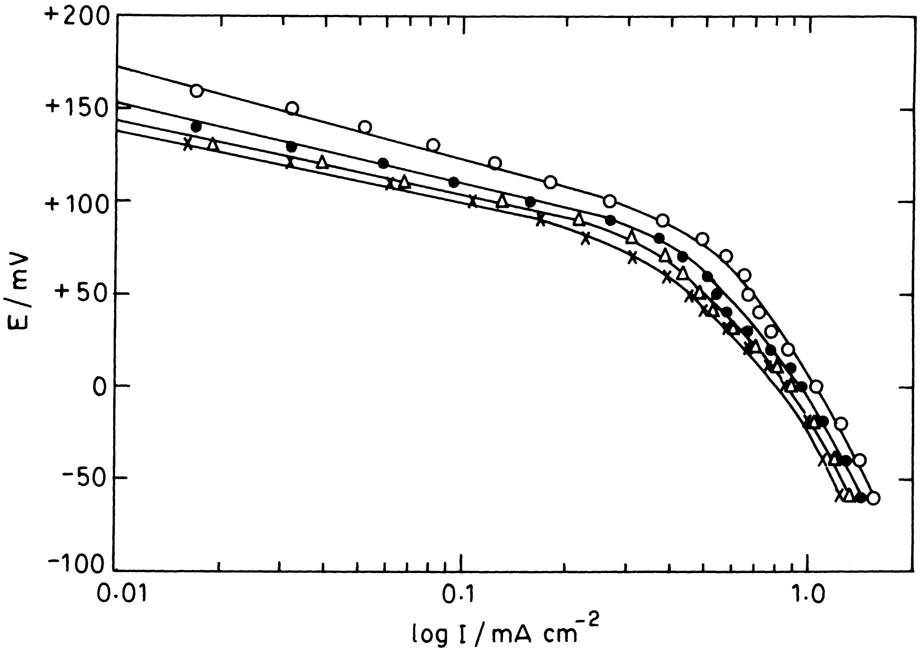

Fig. 3. Tafel plots for oxygen reduction on polystyrene-impregnated $LaNiO_3$ electrode at various KOH concentrations (25 °C): (○) 0.2, (●) 0.5, (△) 0.75 and (×) 1 M.

of electrocatalytic activity, values of i_{app} being 4.8 and 5.6 mA cm^{-2} at $E = 0.525$ V for LN–MA and LN–COP, respectively. In contrast, based on the real surface area of electrodes, the electrocatalytic activity of the LN–MA electrode ($R_F = 1500$) was approximately two times higher than the LN–COP ($R_F = 5600$). The roughness factor (R_F) for the LN–MA electrode has already been determined in [22]. It was noted that in the case of oxygen evolution the true electrocatalytic activity of LN–SP was greatest while that of LN–C was lowest. On the other hand, in the case of oxygen reduction, the LN-MA electrode has the greatest electrocatalytic activity. Its activity was more than 50 times greater than LN–COP. Comparative E against log i plots for different electrodes are shown in Fig. 6.

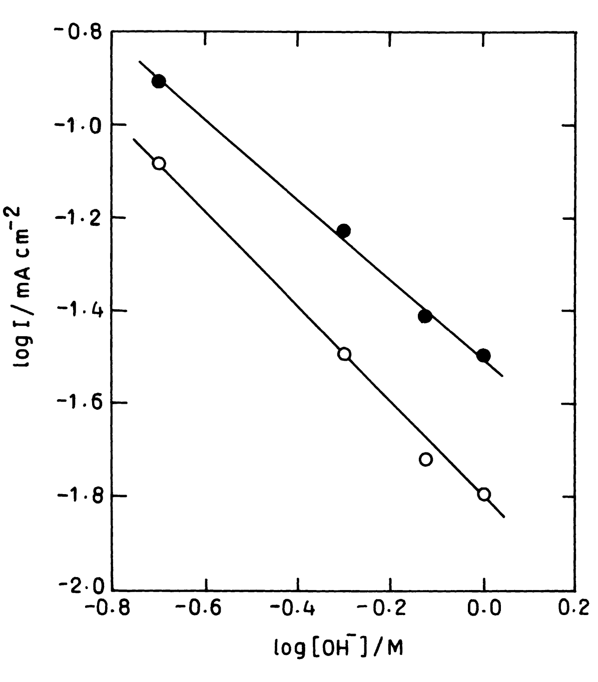

Fig. 4. Plot of log I against log [OH$^-$] from polarization curves in Fig. 3. Key: (●) p = 0.9 (+120 mV); (○) p = 1.0 (+130 mV).

The stability of the electrode was examined by polarizing the electrode anodically for a period of 50 h at 50 mA cm^{-2} in 1 M KOH. This test showed a quite stable potential during the period of investigation (Fig. 7).

5. Conclusion

This study shows that the malic acid-aided method (which is a modified sol–gel route) improves both geometric, as well as electronic, properties of the catalyst favourably. The apparent and true catalytic activity of this catalyst, particularly in the case of electrochemical reduction of oxygen in 1 M KOH, is found to be many times higher than those obtained by other methods. This indicates the possibility of obtaining large-area and catalytically active oxide materials through sol-gel routes.

Acknowledgement

The authors are grateful to the Indo-French Centre for the Promotion of Advanced Research (Centre Franco-Indien pour la Promotion de la Research Avancee), New Delhi, India, for financial support of this work. One of the authors (SKT) is also thankful to CSIR, New Delhi, India for providing financial assistance in the form of a Senior Research Associateship through the Scientist's Pool Scheme to complete a part of the work in India.

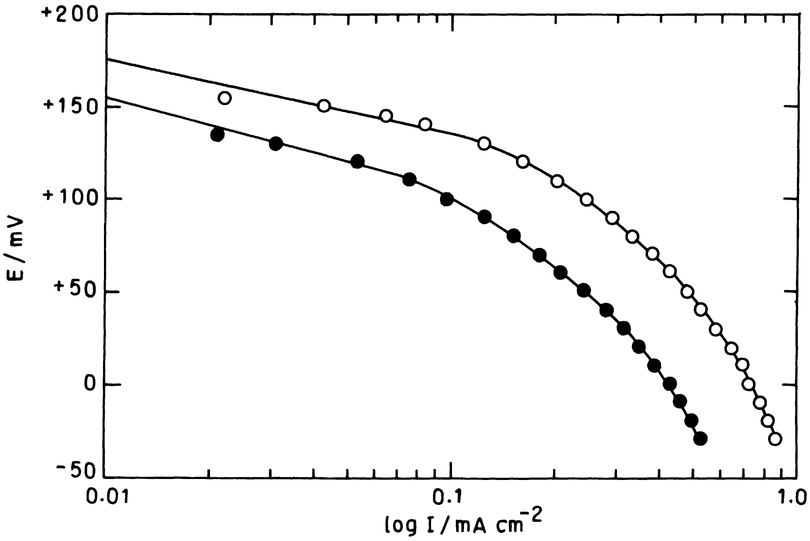

Fig. 5. Influence of oxygen partial pressure on oxygen reduction on polystyrene-impregnated $LaNiO_3$ electrode (25 °C). Key: (○) $P_{O_2} = 1.0$ bar; (●) $P_{O_2} = 0.22$ bar.

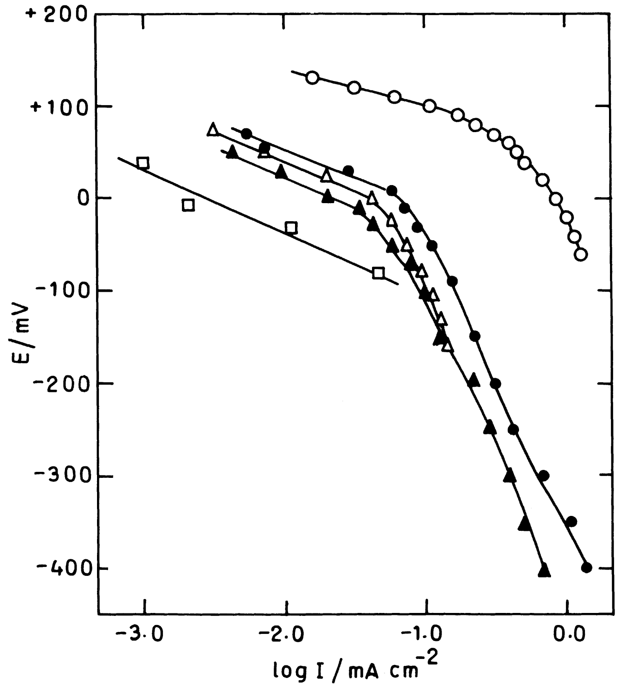

Fig. 6. Comparative Tafel plots for oxygen reduction on different $LaNiO_3$ electrodes and Pt in 1 M KOH (or NaOH) solution; (▲, ●) [11], (□, △) [25]. Key: (□) Pt; (△) $LaNiO_3$ ceramic; (▲) $LaNiO_3$ (multiphase); (●) coprecipitation; (○) malic acid-aided.

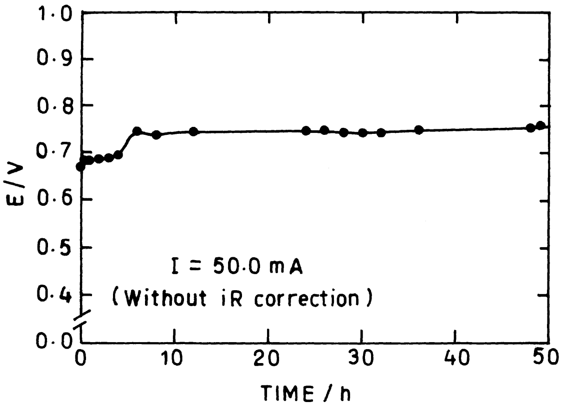

Fig. 7. Performance of the polystyrene-impregnated $LaNiO_3$ electrode in 1 M KOH (25 °C).

References

[1] S. Trasatti (Ed.), 'Electrodes of Conductive Metallic Oxides", Part A and B, Elsevier, Amsterdam (1980).

[2] E. J. M. O'Sullivan and E. J. Calvo, in 'Comprehensive Chemical Kinetics', Vol.27 (edited by R. G. Compton), Elsevier, Amsterdam (1987).

[3] S. Trasatti, *in* 'The Electrochemistry of Novel Materials' (edited by J. Lipkowski and P. N. Ross), VCH, Weinheim (1994).

[4] P. Rasiyah and A. C. C. Tseung, *J. Electrochem. Soc.* **130** (1983) 365; *ibid* **130** (1983) 2384.

[5] J. C. Botejue Nadesan and A. C. C. Tseung, *ibid.* **132** (1985) 295.

[6] R. Boggio, A. Carugati and S. Trasatti, *J. Appl. Electrochem.* **17** (1987) 828.

[7] R. N. Singh, J. F. Koenig, G. Poillerat and P. Chartier, *J. Electrochem. Soc.* **137** (1990) 1408.

[8] S. K. Tiwari, S. Samuel, R. N. Singh, G. Poillerat, J. F. Koenig and P. Chartier, *Int. J. Hydrogen Energy* **20** (1995) 9.

[9] A. G. C. Kobussen, F. R. Van Buren, T. G. M. Van den Belt and H. J. A. Van Wees, *J. Electroanal. Chem.* **96** (1979) 123.

[10] Y. Matsumoto, H. Manabe and E. Sato, *J. Electrochem. Soc.* **127** (1980) 811.

[11] J. O'M. Bockris and T. Otagawa, *ibid.* **131** (1984) 290.

[12] J. Balej, *Int. J. Hydrogen Energy* **10** (1985) 89.

[13] S. K. Tiwari, P. Chartier and R. N. Singh, *J. Electrochem. Soc.* **142** (1995) 148.

[14] R. N. Singh, A. N. Jain, S. K. Tiwari, G. Poillerat and P. Chartier, *J. Appl. Electrochem.* **25** (1995) 1133.

[15] A. N. Jain, S. K. Tiwari, P. Chartier and R. N. Singh, *J. Chem. Soc. Faraday Trans.* **91** (1995) 1871.

[16] S. K. Tiwari, S. P. Singh and R. N. Singh, *J. Electrochem. Soc.* **143** (1996) 1493.

[17] R. N. Singh, S. P. Singh, N. K. Singh, S. K. Tiwari, G. Poillerat and P. Chartier, *J. Chem. Soc. Faraday Trans.* **92** (1996) 2593.

[18] H. Obayashi and T. Kudo, *Jpn. J. Appl. Phys.* **14** (1975) 330.

[19] A. M. Kannan, A. K. Shukla and S. Sathyanarayana, *J. Electroanal. Chem.* **281** (1990) 339.

[20] R. N. Singh, L. Bahadur, J. P. Pandey, S. P. Singh, P. Chartier and G. Poillerat, *J. Appl. Electrochem.* **24** (1994) 149.

[21] S. P. Singh, R. N. Singh, G. Poillerat and P. Chartier, *Int. J. Hydrogen Energy* **20** (1994) 203.

[22] M. El Baydi, S. K. Tiwari, R. N. Singh, J. L. Rehspringer, P. Chartier, J. F. Koenig and G. Poillerat, *J. Solid State Chem.* **116** (1995) 157.

[23] E. J. Calvo, J. Drennan, B. C. H. Steale and W. J. Albery, *Solid State Ionics* (1984) 294.

[24] R. N. Singh, S. K. Tiwari and P. Chartier, *Ind. J. Chem.* **29A** (1990) 837.

[25] Y. Matsumoto, H. Yoneyama and H. Tamura, *Chem. Lett.* (1975) 661.

[26] *Idem*, *J. Electroanal. Chem.* **79** (1977) 319; *ibid.* **80** (1977) 115; *ibid.* **83** (1977) 167, 237, 240.

[27] E. J. Calvo, J. Drennan, J. A. Kilner, W. J. Albery, *Proc-Electrochem. Soc.* 84-12 (Chem. Phys. Electrocatal.), (1984) p. 489.

[28] Y. Matsumoto, H. Yoneyama and H. Tamura, *Bull. Chem. Soc. Jpn.* **51** (1978) 1927.

[29] G. Karlsson, *J. Power Sources* **10** (1983) 319.